



Research article

The use of chitosan in protecting wooden artifacts from damage by mold fungi



Rehab El-Gamal ^a, Efstratios Nikolaivits ^a, Georgios I. Zervakis ^b, Gomaa Abdel-Maksoud ^c, Evangelos Topakas ^a, Paul Christakopoulos ^{d,*}

^a Biotechnology Laboratory, School of Chemical Engineering, National Technical University of Athens, 9 Heroon Polytechniou Str., Zographou Campus, 15780 Athens, Greece

^b Agricultural University of Athens, Laboratory of General and Agricultural Microbiology, Iera Odos 75, 11855 Athens, Greece

^c Conservation Department, Faculty of Archaeology, Cairo University, Giza, Egypt

^d Biochemical and Chemical Process Engineering, Division of Sustainable Process Engineering, Department of Civil, Environmental and Natural Resources Engineering, Luleå University of Technology, SE-97187 Luleå, Sweden

ARTICLE INFO

Article history:

Received 23 April 2016

Accepted 11 October 2016

Available online 26 October 2016

Keywords:

Archeological wood

Chitosan protection

Crystallinity index

Damage of wooden artifacts

Filamentous fungi

FTIR

Fungal damage

Prevention of fungal growth

UV spectrophotometry

Wood deterioration

XRD

ABSTRACT

Background: Many buildings in Egypt e.g. museums, mosques and churches, do not possess controlled environments for minimizing the risks of damage of wooden artifacts due to the growth of fungi. Fungal damage usually appears as change in wood color, appearance of stains, and sometimes deformation of wooden surfaces. In this study we focused on the effect that some fungi exert on the properties of wooden artifacts and evaluated the effectiveness of different concentrations of chitosan on their protection against damage by mold fungi.

Results: Samples were collected from different monuments and environments, and fungi growing on them were isolated and identified. The isolated *Penicillium chrysogenum*, *Aspergillus flavus* and *Aspergillus niger* strains were used for the infestation of new pitch pine samples. The results revealed that the lightness of samples infected with any of the tested fungi decreased with increasing incubation times. XRD analysis showed that the crystallinity of incubated samples treated individually with the different concentrations of chitosan was lower than the crystallinity of infected samples. The crystallinity index measured by the first and the second method decreased after the first and second months but increased after the third and fourth months. This may be due to the reducing of amorphous part by enzymes or acids produced by fungi in wooden samples.

Conclusions: The growth of fungi on the treated wood samples decreased with increasing the concentration of chitosan. Hence, it was demonstrated that chitosan prevented fungal growth, and its use could be recommended for the protection of archeological wooden artifacts.

© 2016 Pontificia Universidad Católica de Valparaíso. Production and hosting by Elsevier B.V. All rights reserved. This is an open access article under the CC BY-NC-ND license (<http://creativecommons.org/licenses/by-nc-nd/4.0/>).

1. Introduction

Wood consists of an orderly arrangement of cells with cell walls composed of varying amounts of cellulose, hemicelluloses, and lignin. The remaining components consist of various extracellular compounds [1]. When exposed to even moderate environmental conditions, wood deteriorates rapidly through a variety of biotic processes [2]. It is important to consider environmental factors such as moisture content, wood temperature, accessible nutrients, and the types of wood-decaying fungi present [3,4]. Fungi are widespread in nature and cause deterioration of wooden artifacts in a range of

terrestrial and aquatic environments [5]. The structure of wood acts as a substrate template for fungal growth and development. During the damage and decay process, fungal hyphae may grow on the wood surfaces and into the wood via the xylem rays and then spread further. Depending on the type of decay, the fungal hyphae may be located in the cell lumen or even within all cell wall layers [3].

Most librarians, archivists, and museum personnel share the conviction that fungi should be eliminated. It is perhaps more appropriate and effective to concentrate on prevention. Here we restrict the meaning of the term fungicide to biocides in glacial acetic acid medium that can be applied directly to the surface of affected wood.

Chitosan has become a vital biocide and is used in different fields because of its high antimicrobial activity against various microorganisms [6]. Special interest has been shown in the use of chitosan for the control of wood degrading fungi. This may be due to

* Corresponding author.

E-mail address: paul.christakopoulos@ltu.se (P. Christakopoulos).

Peer review under responsibility of Pontificia Universidad Católica de Valparaíso.

the fact that chitosan toxicity exerts an effect on membrane permeability and on the architecture of the mycelium [7]. It was found that increasing concentrations of chitosan would cause an increase in chitin deposition, which would reflect changes occurring at morphological and ultrastructural level within the cell wall. Increase of the chitin content in the mycelium in the presence of increasing concentrations of chitosan suggesting that chitosan treatment enhanced deposition of cell wall [8]. It has been used widely due to its biodegradability, biocompatibility, antimicrobial effects, lack of toxicity, and anti-tumor properties [9]. Ahonkhai et al. [10] reported that chitosan is freely available, is cheap, and has antifungal and bacteriostatic properties. Chitin is naturally found in the exoskeleton of crustaceans and insects [11]. Chitosan occurs naturally in fungi of the order Mucorales. Commercial chitosan is mainly obtained by partially removing the acidic acid residues from the chitin of crustaceans. The polymer is characterized as chitosan according to the degree of deacetylation (DD), which is determined from the proportion of D-glucosamine and N-acetyl-D-glucosamine. Structurally, chitosan is a straight-chain copolymer composed of D-glucosamine and N-acetyl-D-glucosamine. It is the most abundant basic polymer and is structurally similar to cellulose, which is composed of only one monomer (glucose). The solubility of chitosan depends on the amount of protonated amino groups in the polymeric chain, and therefore on the proportion of acetylated and non-acetylated D-glucosamine units. It is soluble after stirring in acids such as acetic, nitric, hydrochloric, perchloric, and phosphoric [12,13,14,15,16,17,18,19]. In recent years, chitosan has been investigated as a chemical for protection of wood against fungal decay. Schmidt et al. [20] found that 2% chitosan treatment decreased the wood decay by two brown-rot fungi considerably. It has been used in aqueous solution, employing an impregnation technique [21].

Analyses and investigations are considered to be the most important tools for evaluation of the environment, and of materials that are used in conservation processes. The X-ray diffraction method has been used more and more extensively in the past twenty years for the characterization of different crystalline and non-crystalline materials of archeological, historical, and artistic interest [22]. Abdel-Maksoid and Al-Saad [23], Abdel-Maksoud [24], and Marutoiu et al. [25] have used X-ray diffraction for the determination of wood crystallinity. Bugheanu et al. [26], Picollo et al. [27], and Gelbrich et al. [28] have used FTIR for determination of the extent of deterioration of wood. Lo Monaco et al. [29] and Ozgenc et al. [30] have used UV spectrophotometry for measurement of color changes of wood treated with different applications.

In this study, we aimed to:

- Isolate and identify mold fungi from monuments in different locations and environments of historical Cairo;
- Study the effects of mold fungi that were isolated and identified on selected properties of pitch pine wood;
- Evaluate the efficiency of different concentrations of chitosan for the protection of wood from mold fungi.

2. Materials and methods

2.1. Archeological samples

The fungi studied were isolated from the following sites:

- The Mosque of Sabiile and Koutab Suleiman Agha Selehdar, which is located in El Muizz Street, Islamic Cairo. It was established in 1837–1839 AD (1253–1255 AH).
- The Mosque of Abu Haribh, which was built by Prince Sayf al-Din Akjmas Ishaqi El Zahery between 1480 and 1481 AD (885–886 AH).
- The Mosque of El Musafir Khana, situated at Darb Almsmt, El Gamaliya, and created by Mahmud Muharram. The first section was built in 1779 AD (880 AH), and the second in 1783 AD (884 AH).

- The Mosque of El Mouayed Sheikh Al-Mahmoudi, Inside Bab Zuwayla, close to the El Soukary neighborhood. The construction of the mosque took about six years, from 1415 to 1421 AD (818–824 AH).

2.2. Isolation and identification of fungi

Isolation of fungi was done according to Abdel-Maksoud [24]. Pieces of deteriorated wood were placed into sterile plastic bags and were transferred to the laboratory, where their inner parts were exposed and sterile swabs were used to wipe along surfaces contaminated with fungi. The swabs were then gently wiped onto the surface of a potato-dextrose agar (PDA) medium in Petri dishes, and cultures were incubated at 28°C for 1–2 weeks. Individual fungal colonies were then recovered and transferred to Petri dishes with malt extract agar (MEA). Colonies from the established subcultures were used for the assessment of the morphological characteristics of the isolated fungi [31,32] and for their grouping into distinct species/morphotypes.

In addition, and for verifying initial taxonomic determinations based on morphological features, total genomic DNA of representative strains from each species/morphotype was extracted from mycelium. For the isolation of fungal DNA, 50 mL of potato-dextrose medium were inoculated by stock cultures, which were grown on MEA slants for 7 d at 27°C. Biomass was obtained after 2 d incubation at 27°C by centrifugation at 4000 × g for 10 min and washed twice with double distilled sterile water. Disruption of the cells was performed in a ceramic mortar using liquid nitrogen and a pestle until a white powder was obtained. Genomic DNA was extracted from 100 mg of biomass powder as instructed by the GenElute™ Plant Genomic DNA Miniprep Kit (Sigma-Aldrich, St Louis, MO, USA). Elution was performed in two steps (100 µL each) and the presence of genomic DNA was realized by 1% agarose-gel electrophoresis.

PCR primers used by White et al. [33] design the amplification reactions for the ITS1-5.8S-ITS2 rDNA region were ITS1 (5'-TCCGTAGG TGAACCTGCGG-3') and ITS4 (5'-TCCTCCGCTTATTGATATGC-3'), which were constructed by Eurofins Genomics (Ebersberg, Germany). The following PCR conditions were used for ITS amplification: the reaction was initiated at 95°C for 2 min followed by 35 cycles of 95°C for 20 s, 48°C for 30 s, 70°C for 15 s with a final extension step at 70°C for 2 min. PCR products were checked by agarose-gel electrophoresis using 1 kb DNA Ladder RTU (NIPPON Genetics EUROPE, Düren, Germany). The PCR products were directly sequenced by Eurofins Genomics (Ebersberg, Germany). All fragments were read in both directions and nucleotide sequences were submitted to GenBank database and their accession numbers are the following: KU243044, KU243045, KU243046 and KU243047.

Alignment of sequences was carried out through the use of the Clustal Omega software (<http://www.clustal.org/omega/>). Phylogenetic relationships were inferred by using the Maximum Likelihood method based on the Kimura 2-parameter model [34]. Initial tree(s) for the heuristic search were obtained by applying the Neighbor-Joining method to a matrix of pairwise distances estimated by the Maximum Composite Likelihood (MCL) approach. The branch swap filter was set at 'strong', and all sites were used for the analysis including gaps. Bootstrap values were derived from a total of 10,000 replicates. Pertinent analyses were conducted through the use of MEGA 6 software [35]. Eleven additional sequences from related (to this study's material) fungal taxa were retrieved from GenBank, and were included in the phylogenetic analysis. Among them, *Mucor fragilis* was used as outgroup.

2.3. Fungal strains

In this study, the three active strains *Aspergillus niger*, *Aspergillus flavus*, and *Penicillium chrysogenum* were isolated from wood samples taken from the different locations mentioned above.

2.4. Inoculation of wood samples with the isolated fungi

For fungal growth prior to infestation of wood samples, Czapek-Dox agar (CZA) was used: sucrose 30 g/L, sodium nitrate 2 g/L, dipotassium phosphate 1 g/L, magnesium sulfate 0.5 g/L, potassium chloride 0.5 g/L, ferrous sulfate 0.01 g/L, agar 20 g/L (final pH: 7.3 at 25°C). CZA was poured into Petri dishes, and was further inoculated with fungal spores, which were uniformly distributed onto the medium surface by a wrapped glass spreader, and wood samples (treated and untreated, with and without fungicide) were put at the center of each petri dish. Petri dishes were sealed by using Parafilm to prevent any possible contamination and drying of agar during an incubation period of four months at 28°C.

2.5. Sample incubation

Fungal cultures were incubated at 28°C for four months. After this incubation period, the wood samples were picked out and cleaned mechanically with a brush to remove mycelia. The samples were conditioned at $21 \pm 2^\circ\text{C}$ and 65% relative humidity (RH) for 72 h before measurements.

2.6. The application of fungicide to the wood samples

The application method used was the impregnation technique. The samples were soaked until saturation with fungicide. Upon removal of excess fungicide, the samples were allowed to dry at the room temperature, and then were transferred to Petri dishes [36]. Chitosan [deacetylated chitin, poly(D-glucosamine)] dissolved in 2% acetic acid was used in this study. The concentrations used were 0.25%, 0.50 % and 0.75%. Chitosan (low molecular weight) was purchased from Aldrich. The control samples were treated with acetic acid (2%) alone.

3. Investigation techniques

3.1. Measurement of color change with UV spectrophotometry

Color changes caused by the effect of accelerated incubation cycles were measured by using the CIE $L^*a^*b^*$ system [23,37,38]. The L^* scale measures lightness, and varies from 0 (black) to 100 (perfect white). The a^* scale measures red-green, with '+a' meaning more red and '-a' meaning more green. The b^* scale measures yellow-blue, with '+b' meaning more yellow and '-b' meaning more blue. The total color difference (ΔE) is calculated according to Equation 1 [39]:

$$\Delta E = \sqrt{(\Delta L)^2 + (\Delta a)^2 + (\Delta b)^2} \quad [\text{Equation 1}]$$

Measurements were made using a Macbeth Color Eye 7000 UV spectrophotometer (Gretag Macbeth, USA).

3.2. Fourier transform infrared spectroscopy (FTIR)

Fourier transform infrared attenuated total reflection spectroscopy (FTIR-ATR) has been used extensively to investigate adsorption and reactions on surfaces. This method of analysis was used in accordance with Jadoul et al. [40], Pouliot et al. [41], Xie et al. [42], Velkova and Lafleur [43], Kazarian and Chan [44], Liao et al. [45], Dias et al. [46], and Russeau et al. [47]. A significant advantage of the ATR technique is that the wood sample does not require any preparation, thereby minimizing possible damage to the sample [48]. The infrared spectra were obtained using a JASCO-ATR-FT/IR-6100 Fourier transform infrared spectroscopy.

3.3. XRD for the determination of wood crystallinity

The crystallinity of selected samples that were either untreated or treated with chitosan at different concentrations, and of samples infected by the fungi under study, was determined using a Lab XRD 6000 X-ray diffractometer (Shimadzu, Japan). The results for four peaks were selected in the fitting of each diffractogram, three peaks for the cellulose crystalline peaks (101), (10 $\bar{1}$), and (002) peaks. In this study, the position (2θ degrees), the full width at half maximum (FWHM) (2θ degrees), and intensity were obtained for each fitted peak.

3.3.1. Peak position (2θ degrees)

The positions of the peaks in an X-ray diffractogram reflect the dimensions of the crystallite of the cellulose unit cell.

3.3.2. Peak width (2θ degrees)

Measurement of the degree of crystallinity by using peak width (the width at half height parameters in 2θ degrees) was done in accordance to Hermans and Weidinger [49]. The peak width was calculated by taking the difference between the peak position and the half height intersection, and multiplying by two. These parameters should represent the width of the peak at half its height if no other peaks have interfered.

3.3.3. Peak intensity (2θ degrees)

There are two methods for evaluation of the intensity of untreated, incubated and untreated, and incubated and treated wood samples. These methods were applied as follows:

3.3.3.1. First method. This method was used in accordance with Hermans and Weidinger [49]. In this method, the intensities of the (10 $\bar{1}$) and (002) peaks were normalized against the (101) peak intensity.

3.3.3.2. Second method. This method was used in accordance with Segal et al. [50] and Terinte et al. [48]. By this method, the crystallinity index can be calculated according to Equation 2:

$$\text{CrI} = \left[\frac{I_{002} - I_{am}}{I_{002}} \right] * 100 \quad [\text{Equation 2}]$$

where CrI is the crystallinity index, I_{002} is the intensity at approximately $22.6^\circ 2\theta$ and I_{am} is the intensity at approximately $19^\circ 2\theta$.

This crystallinity index, which is based on the two-phase model for cellulose, has no absolute theoretical significance, but it is as good as any other approach for the relative ranking of cellulose I crystallinities. This method was therefore used in ranking the crystallinities of the cellulose examined.

4. Results and discussion

4.1. Identity of the fungal strains isolated from wooded artifacts

The main morphological features of the strains isolated were as follows:

- Strain HRa – MEA 25°C, 7 d: colony diameters 8.5–9.0 cm, plane to floccose; conidial heads radiate to columnar, yellowish to green to olive green; mycelium white; reverse uncolored. Stipes 160–730 × 6.4–21.5 μm , rough, pale brown; vesicles globose to subglobose to ellipsoidal, 20.5–55.0 μm wide. *Aspergilla* biseriata, less of tenuniseriate, or both in the same vesicle; metulae 8.0–15.4 × 3.7–7.2 μm , phialides 7.6–13.0 × 2.2–4.4 μm ; conidia globose, smooth to finely rough, 3.8–5.9 × 2.7–3.3 μm .
- Strains A2 and HRb – MEA 25°C, 7 d: colony diameters 8.5–9.0 cm, granular, conidial heads radiate or splitting into columns, brownish

olive to green brown, later dark brown to black; mycelium white, submerged; reverse color cream. Stipes 330–2300 × 4.8–21.5 μm, uncolored to light brown, smooth; vesicles globose, 25.0–70.0 μm wide. *Aspergilla* biseriolate; metulae rarely septate, 12.8–36.0 × 4.2–10.4 μm; phialides 5.7–11.6 × 2.9–4.4 μm. Conidia subglobose to globose, rough, 3.3–5.5 × 2.6–5.1 μm.

- c) Strain 503 – MEA 25°C, 7 d: colony diameters 30–35 mm, plane, velutinous, margin entire, mycelium white, margin thin; conidiogenesis abundant, grayish green to dull green; no exudates or soluble pigments; reverse yellow to dull green. Conidiophores borne from aerial and superficial mycelium; stipes septate, apices vesiculate, 45–130 × 3.4–3.7 μm, smooth, thin walled; penicilli mostly irregularly terverticillate or quaterverticillate; metulae in verticils of 2–6, smooth, 7.4–13.0 × 2.4–5.2 μm; phialides in verticils of 5–9, ampulliform, smooth, 6.8–7.2 × 2.5–2.8 μm; conidia subglobose to broadly ellipsoidal, 2.5–3.1 × 2.4–2.8 μm, smooth, thick walled, borne on long irregular columns.

The above morphological descriptions led to the following initial taxonomic assessments: *A. flavus* for strain HRa, *A. niger* for strains A2 and HRb, and *P. chrysogenum* for strain 503.

Since identification to species level for fungi of these two genera is often difficult and ambiguous, the four strains were also subjected to sequence analysis of their ITS-5.8S region. The obtained sequences (GenBank accession numbers: KU243044, KU243045, KU243046 and KU243047) were compared to published sequences selected on the basis of their highest homology (99–100%, through the use of the BLASTN algorithm, NCBI). The phylogenetic tree constructed by including all these sequences confirmed the identity of the three out of the four strains examined, while the fourth strain (HRb) was grouped together with *A. tubingensis* (Fig. 1). It is noteworthy that *A. niger* and *A. tubingensis* are among the several morphologically indistinguishable species of the section *Nigri* [51,52]; hence, the use of molecular markers was necessary for their discrimination [53].

4.2. Change of color

4.2.1. Lightness (L^* value)

It was clear from the data obtained (Table 1) that the lightness of the samples infected by the isolated fungi decreased in relation to those of the control samples, and also decreased with increasing the incubation times. The highest reduction in lightness was obtained by *A. niger*, followed by *P. chrysogenum* and *A. flavus* respectively.

The data obtained from the incubated sample treated with chitosan revealed the resistance of the sample to fungal infection. The concentration of chitosan plays an important role against the fungi studied and at improving lightness compared to infected samples without treatment. The best results of lightness were obtained from the third concentration, followed by the second and the first concentrations respectively. It should be mentioned that the ability of chitosan for disinfection decreased with increasing the incubation times.

4.2.2. Hue: more red (a^* value)

It was clear from the data obtained (Table 1) that the degree of red color of the infected samples by fungi studied increased with high degree compared to the control sample. The results revealed that the degree of red color (a^* value) of infected samples decreased with increasing incubation time until the 4th month of incubation. The highest increasing in red color value was obtained from *P. chrysogenum*, followed by *A. niger* and *A. flavus* respectively.

It was also noticed that the red color of the treated samples decreased compared to the infected samples by fungi. The reduction of red color of the treated samples decreased with increasing the concentration of chitosan. It should also be mentioned that the red color value of the treated and infected by fungi samples increased with increasing the incubation times at all concentrations used.

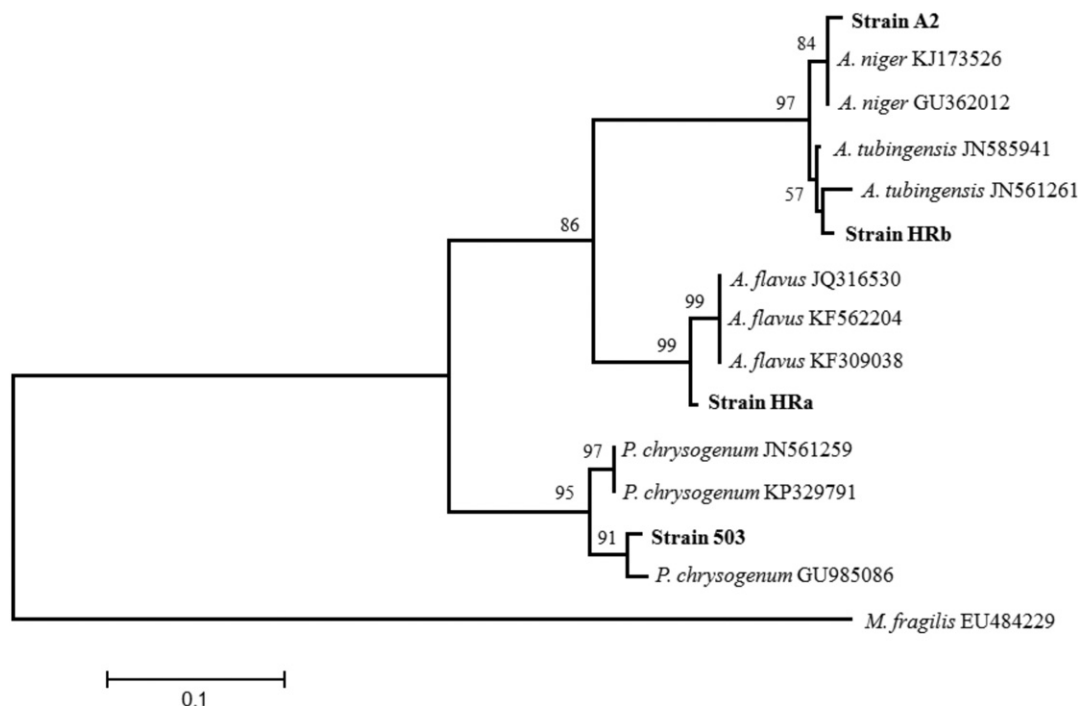


Fig. 1. Phylogenetic relationships among fungal strains of the genera *Aspergillus* and *Penicillium* isolated from the inner part of wooden artifacts as inferred by using the Maximum Likelihood method based on the Kimura 2-parameter model [34]. The tree with the highest log likelihood (-3274.0695) is shown. Sequences derived in the frame of the present study are marked in bold, whereas other highly-similar sequences were obtained from the GenBank. The percentage of replicate trees in which fungal material clustered together in the bootstrap test (10,000 replicates) are shown next to the branches when values $\geq 50\%$ [63]. *Mucor fragilis* was used as outgroup.

Table 1
Change of color of wood samples treated with chitosan at different concentrations against infection by selected strains of *A. flavus*, *A. niger* and *P. chrysogenum*, and their subsequent incubation for 1, 2, 3 and 4 months.

Samples	<i>A. niger</i>				<i>A. flavus</i>				<i>P. chrysogenum</i>			
	Color values			Total color difference ΔE	Color values			Total color difference ΔE	Color values			Total color difference ΔE
	L	a	b		L	a	b		L	a	b	
Incubation: 1 month												
Control	67.20	6.48	27.63	0.0	67.16	6.84	27.63	0.0	67.16	6.84	27.63	0.0
Infected sample before treatment	49.30	13.96	25.20	57.10	54.34	18.54	33.70	66.57	51.40	13.50	30.30	61.17
Treated sample (0.25%)	63.70	6.20	27.10	69.50	65.17	6.30	27.20	70.90	64.50	6.10	27.01	70.19
Treated sample (0.50%)	65.40	6.40	27.31	71.17	66.85	6.40	27.93	72.73	65.90	6.35	27.30	71.61
Treated sample (0.75%)	66.80	6.55	27.47	72.50	67.03	6.70	27.50	72.76	66.70	6.42	27.44	72.40
Incubation: 2 months												
Control	67.16	6.84	27.63	0.0	67.16	6.84	27.63	0.0	67.16	6.84	27.63	0.0
Infected sample before treatment	40.20	10.52	23.30	27.73	45.20	16.20	35.41	25.11	46.20	12.20	28.23	21.64
Treated sample (0.25%)	62.98	5.87	26.20	4.52	64.81	5.41	27.94	2.77	63.85	5.79	26.45	3.51
Treated sample (0.50%)	64.59	6.02	25.94	3.18	66.21	5.99	27.88	1.14	64.76	5.98	26.45	2.81
Treated sample (0.75%)	65.71	6.12	25.41	2.75	66.20	6.10	27.70	1.21	66.19	5.55	26.65	1.89
Incubation: 3 months												
Control	67.16	6.48	27.63	0.0	67.16	6.84	27.63	0.0	67.16	6.84	27.63	0.0
Infected sample before treatment	34.20	7.57	19.50	33.96	40.15	-10.20	42.02	30.97	39.98	7.30	31.52	27.46
Treated sample (0.25%)	60.51	5.02	25.42	7.13	62.97	4.78	28.70	4.79	61.89	4.89	26.20	5.80
Treated sample (0.50%)	63.80	5.57	25.01	3.81	64.04	5.12	28.20	3.61	63.08	5.11	25.80	4.79
Treated sample (0.75%)	64.59	5.88	24.80	2.91	65.31	5.45	27.80	2.32	64.46	5.23	25.48	3.81
Incubation: 4 months												
Control	67.16	6.48	27.63	0.0	67.16	6.84	27.63	0.0	67.16	6.84	27.63	0.0
Infected sample before treatment	29.80	5.40	13.24	40.06	34.51	-14.54	46.20	38.34	32.98	5.26	34.56	34.91
Treated sample (0.25%)	58.11	4.95	24.15	9.88	58.30	4.20	26.70	9.29	57.70	4.26	28.10	9.82
Treated sample (0.50%)	60.41	5.20	23.70	7.98	61.40	4.92	26.20	6.24	59.10	4.89	27.70	8.29
Treated sample (0.75%)	61.50	5.61	23.10	7.35	61.95	5.10	25.90	5.76	60.56	5.02	27.13	6.86

4.2.3. Hue: more yellow (b^* value)

It was clear from the data obtained that the b^* value of the infected sample corresponded to yellow, which increased by increasing the incubation time. The highest increasing in red color value was obtained from *P. chrysogenum*, followed by *A. niger* and *A. flavus*, respectively.

The yellow color of the samples treated with chitosan increased with all chitosan concentrations and with all incubation times, relative to the control samples. The yellow color value of treated samples with chitosan decreased compared to the infected samples by fungi without treatment. The yellow color value of the treated samples decreased with increasing the concentration of chitosan. The results confirm that the yellow color value of the treated and infected by fungi samples increased with increasing the incubation times at all concentrations used.

4.2.4. Total color difference (ΔE)

It was clear from the data obtained that the total color difference in the infected samples increased with increasing incubation time. The total color difference in the treated samples decreased with increasing concentration of chitosan.

Mold fungi cause discoloration of wood. Blanchette [3] mentioned that these fungi do not degrade lignified cell walls, but use the contents of ray parenchyma cells to grow on the wood surfaces and slightly into the wood. He also stated that staining fungi have pigmented mycelia that penetrate into the wood through the rays, bordered pits, and cell lumen.

Morrell and Smith [54] observed that the graying of wood surface is almost exclusively the result of growth of dark-colored fungi. The fungi that colonize weathered wood surfaces can grow on most carbon-containing materials. Growth of molds occurs after spores germination on the wood surface; then hyphae ramify through the outer few millimeters of wood by penetrating the cell lumina, bordered pits, and rays. The hyphae of fungi that colonize softwoods are most prominent in rays and resin ducts where they grow by metabolizing sugars, starch, and resin acids. The walls of the ray

parenchyma and epithelial cells surrounding resin ducts are often destroyed, leaving elongated, open channels that increase the permeability of the affected wood. This effect may contribute to pronounced fluctuations in the surface moisture content of wood.

4.3. FTIR analysis

It was clear from the data obtained (Fig. 2) that the band at approximately 3572 cm^{-1} (control sample) could be assigned to O—H stretching vibration, which gives considerable information about the hydrogen bonds. Relative to the control samples and with all incubation times (from 1 month to 4 months), the peak characteristics of hydrogen bonds from the spectra of amorphous cellulose became sharper and of lower intensity, and the peak shifted to higher wavenumber values for all incubated, treated samples at different chitosan concentrations and with all the fungi studied. Compared to the control samples, the wavenumber of the infected samples shifted to lower values with *A. flavus*, and to higher values with *A. niger* and *P. chrysogenum*. Ciolacu et al. [55] stated that the broad band in the $3600\text{--}3100\text{ cm}^{-1}$ region, which is due to OH-stretching vibration, gives considerable information about the hydrogen bonds. The peak characteristics of hydrogen bonds from the spectra of amorphous cellulose became sharper and of lower intensity compared to the initial cellulose samples. Shang et al. [56] stated that the FTIR spectra of wood samples with fungal decay show large changes in peak intensity and peak position, compared to corresponding samples without fungal decay.

For all samples studied and with all incubation times, the band at approximately 2941 cm^{-1} was assigned to the C—H stretching vibration. This peak also shows the presence of amorphous cellulosic samples. With all the fungi studied and with all incubation times, the peak intensity from the incubated samples treated with chitosan decreased relative to those from the control samples and the infected samples. Bugheanu et al. [26] mentioned that the cellulose components are susceptible to microorganisms. Free cellulosic components are a favorite substrate for microorganisms, and a decrease in the corresponding peak intensity is always properly assigned to this phenomenon.

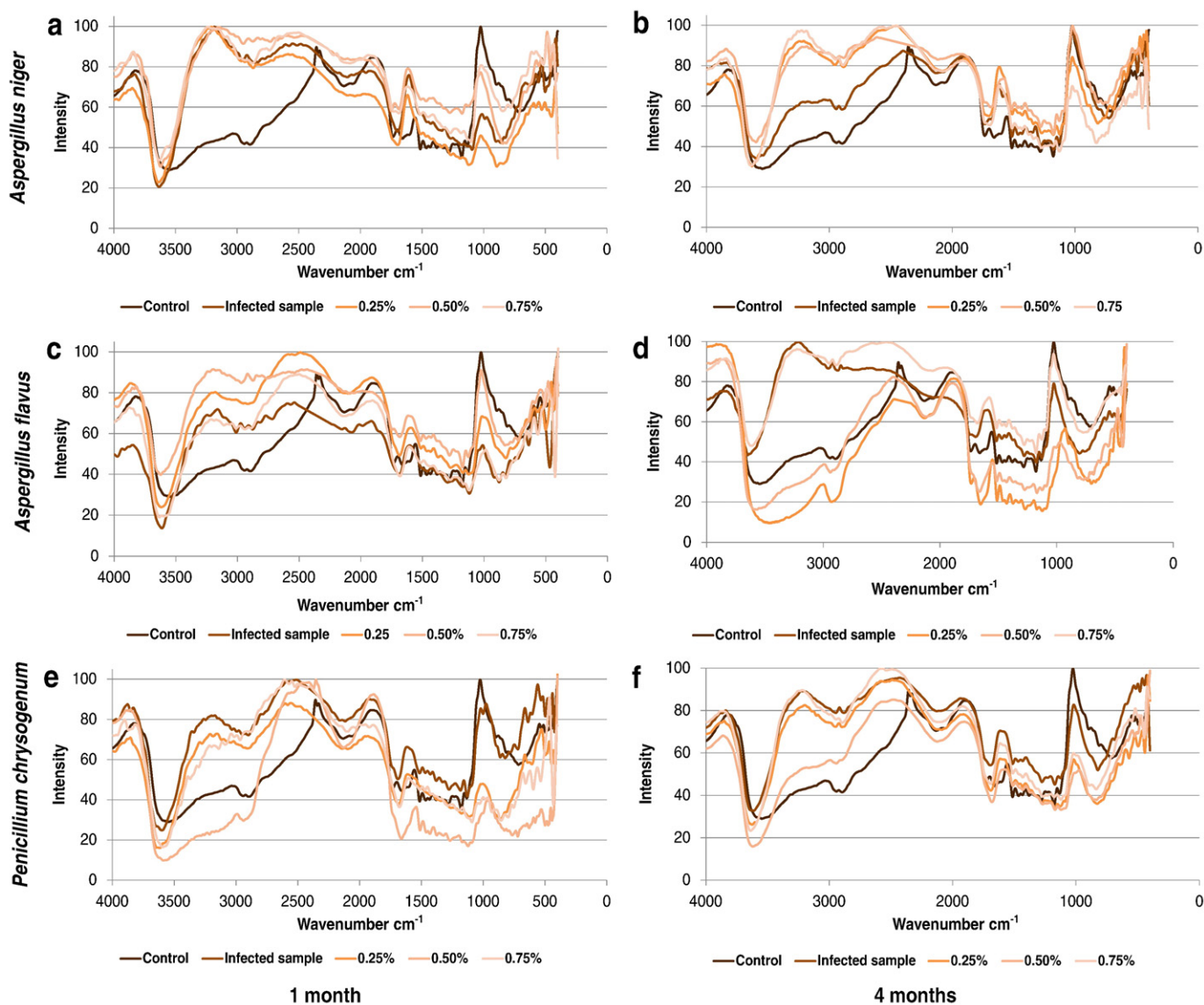


Fig. 2. FTIR of wood samples treated with chitosan at different concentrations against infections by *A. niger*, *A. flavus* and *P. chrysogenum* for incubation periods of 1 month (i, iii, v) and 4 months (ii, iv, vi), respectively.

Lojewska et al. [57] stated that the intensity of the band at around 2900 cm^{-1} comes from the C—H stretching vibrations, which can change depending on the conditions used. In this study, the amount of amorphous cellulose increased with increasing concentration of chitosan.

The bands at 1659 cm^{-1} for the control samples and 1685 cm^{-1} for the infected samples were assigned to C=C bonds. The intensity of this peak from the infected samples increased compared to the peak from the control samples. It also increased with increasing incubation time. The intensity of the band increased because of the appearance of C=C bonds, which indicated that there was a decomposition process. For incubated, treated samples, the intensities of the peak decreased compared to the control samples, and this also indicated the potency of chitosan against infection by the fungi studied. Bugheanu et al. [26] reported that changes in the band at approximately 1650 cm^{-1} are due to the different moisture levels in the samples. The source of moisture in the samples studied may be from the wood samples and chitosan, which was dissolved in 2% acetic acid.

The FTIR absorption band at approximately 1434 cm^{-1} for the control samples, 1428 cm^{-1} for infected samples, and 1424 cm^{-1} for most of the

incubated, treated samples were assigned to an asymmetric CH_2 bending vibration. This band is known as the “crystallinity band”, meaning that a decrease in its intensity reflects a reduction in the degree of crystallinity of the samples. We noticed that the intensity of the band at 1428 cm^{-1} for most of the incubated samples treated with chitosan increased more than with the control samples and infected samples. This band reflects the increase in amorphous cellulose.

4.4. XRD analysis of wood treated with chitosan and infected with different fungi

Poletto [58] explained that there are several ways for the cellulose chains to crystallize. The degree of crystallinity of native cellulose is source-dependent; the crystallinity of wood cellulose is typically around 60%. There are six known crystal polymorphs of cellulose: I, II, III, IIII, IV, and IVIII. In nature, polymerization and crystallization of cellulose occurs simultaneously and its native crystalline form with parallel chains is called cellulose I. The study focuses on cellulose I.

4.4.1. Peak position (2θ degrees)

It was clear from the data obtained (Fig. 3) that the position of the (101), (10 $\bar{1}$) and (002) peaks of the control sample was at 14.4, 16.4 and 22.58 (2θ) respectively. The position of this peaks after infection with any of the fungi studied shifted to a lower value with all incubation times (from 1 to 4 months).

The results revealed that the value for the position of the (101), (10 $\bar{1}$) and (002) peaks increased after treatment with chitosan (with all concentrations) and infected with all fungi studied compared to the control sample. It was also noticed that the increasing of the peaks positions (101), (10 $\bar{1}$) and (002) of the treated samples and infected increased with increasing the concentration of chitosan.

4.4.2. Peak width

The peak width at half maximum is a measurement of the degree of crystallinity of a material. It was clear from the data obtained (Fig. 3) that the peak width for cellulose I ((101), (10 $\bar{1}$), and (002)) of the control sample were 0.09, 0.08, and 0.4 mm, respectively. The peak widths for samples infected with fungi studied increased relative to the control sample. The increasing of the peak width of infected samples increased with increasing the incubation times (from 2 to 4 months). The peaks' width of the treated and infected with fungi samples increased compared to the control and infected samples without treatment. The increasing of the peak width of the treated and infected samples increased with increasing the concentrations of chitosan. It can be said that the samples treated and infected with any of the fungi led to an increase in the peak width, which may have been due to the water used as a solvent with chitosan. The increase in peak width reduced, maybe due to the reduction of wooden samples moisture, after the third and fourth months of incubation.

4.4.3. Peak intensity

From the data obtained (Fig. 3), the crystallinity of the control sample was 3.6 by the first method and 51.4 by the second method. This value decreased after infection with the fungi under study. The decreasing of intensity increased with increasing the incubation times, and this may due to the fact that mold fungi cause microstructural changes of cellulose and reduce the crystallinity values (in those cases that lignin has been already degraded by other fungi).

The crystallinity index of the treated samples and infected with fungi was higher than the control and infected samples without treatment at the first concentration (0.25%). The crystallinity index by the first and second methods decreased after 2 months and started to increase again after the third and fourth months. It was noticed that the crystallinity index by measurement of peak intensity decreased with increasing the concentrations of chitosan. Goh et al. [59] showed that the crystalline phase of cellulose without any microbial infection has a higher intensity than cellulose that has been infected.

5. The application of chitosan on historical wooden artifacts

The impregnation technique was carried out for the application of chitosan on wooden samples in order to obtain information on the effectiveness of this polysaccharide against fungal growth. However, regarding the controls used it must be stated that acetic acid alone inhibits microorganisms. Acetic acid, either chemically pure or as vinegar is one of the oldest and most widespread preservatives of animal feed and food against bacteria, fungi and yeasts. Concentrations of 0.02–0.04% inhibit several bacteria and 0.02–0.09% are lethal; the yeast *Saccharomyces cerevisiae* is inhibited by 0.59% acetic acid and the mold fungus *A. niger* by 0.27% [60].

Samples of the bamboos *Bambusa stenostachya* and *Thyrsostachys siamensis* did not mold after dipping in solutions of 10% acetic acid [61]. Samples of oil and date palm woods treated with 2% acetic acid and then infected with *A. niger* were totally free from fungal growth [62].

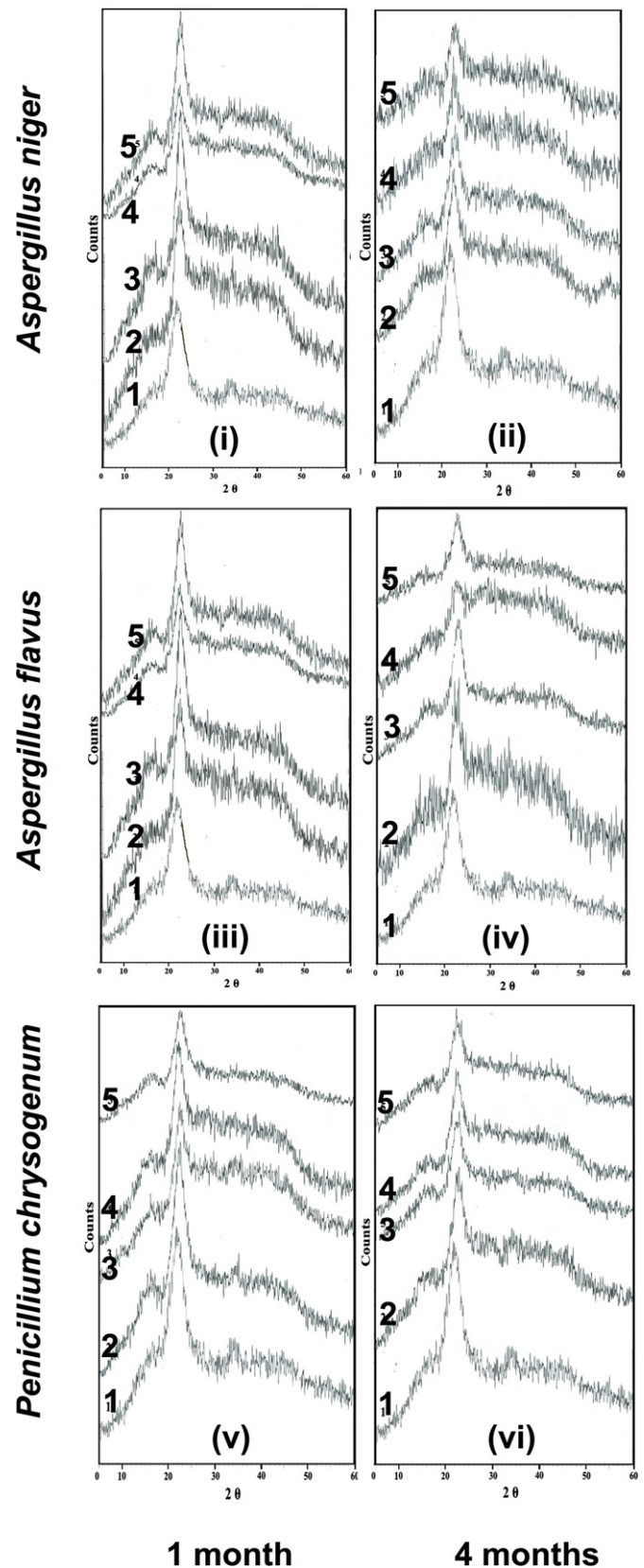


Fig. 3. X-ray diffraction patterns of wood samples treated with chitosan at different concentrations against infections by *A. niger*, *A. flavus* and *P. chrysogenum* (1: control sample, 2: infected sample, 3: treated 0.25% and infected, 4: treated 0.50% and infected, 5: treated 0.75% and infected) for incubation periods of 1 month (i, iii, v) and 4 months (ii, iv, vi), respectively.

However, this technique should not be performed on archeological wooden artifacts. The most suitable technique will depend on the size of wooden artifacts and their state. For example, if the sample has good strength, a soft brush can be used for the application of chitosan, while in the case of sensitive wooden artifacts; the spray technique could be followed.

6. Conclusions

The lightness of the samples infected with any of the fungi studied decreased with increasing incubation time. The resistance to fungi of the samples treated with chitosan increased with increasing concentration of fungicide. The percentage loss of lightness with *A. niger* infection and treatment of samples with chitosan at different concentrations was higher than the percentage loss of whiteness in similarly treated samples infected with *A. flavus* or *P. chrysogenum*. *A. flavus* gave the highest increase in a^* value for the samples treated with chitosan at any of the concentrations used, followed by *P. chrysogenum* and then *A. niger*. The a^* value of the samples treated with chitosan decreased with increasing concentrations of chitosan, but the samples treated at all concentrations had a higher a^* value than the control samples. Yellowness (b^* value) of samples infected with fungi increased with increasing incubation time. The yellowness of the samples treated with chitosan was higher than that of the control samples, but this value decreased with increasing concentrations of chitosan after one month with all the fungi studied, after two months with *A. flavus*, and after three months with *A. niger* and *A. flavus*.

FTIR analysis showed that treatment of wood with the fungicide chitosan conferred resistance to fungal growth, since the intensity of the band at 1685 cm^{-1} for the infected samples, assigned to C=C bonds, increased more than for the incubated, treated samples, irrespective of incubation time. FTIR analysis confirmed that for all fungi studied, incubated samples treated with chitosan were more amorphous during the incubation times than the infected samples.

X-ray diffraction analysis showed that with all the fungi studied, the peak positions of cellulose I ((101) , $(10\bar{1})$ and (002)) in infected samples decreased compared to the control samples during all incubation times. The peak positions of the incubated, treated samples increased with increasing concentration of chitosan. The X-ray diffraction analysis proved that after the first and second months, the peak position and peak width increased after chitosan treatment and infection with any of the fungi. This increase decreased after the third and fourth months, but was still higher than for the control sample. The crystallinity index, measured with either the first or the second method, decreased, but increased after the third and fourth months of incubation with any of the fungi studied. The highest concentration of chitosan tested (0.75%) conferred high resistance to fungal growth, and this concentration can be recommended for use with historical wooden artifacts.

Financial support

Rehab El-Gamal work was supported by grant from the Hellenic State Scholarships Foundation. Paul Christakopoulos would like to thank Bio4Energy, a Strategic Research Environment appointed by the Swedish Government for supporting this work.

Conflict of interest

The authors declare no conflict of interest.

References

- Blanchette RA. A review of microbial deterioration found in archaeological wood from different environments. *Int Biodeter Biodegr* 2000;46:189–204. [http://dx.doi.org/10.1016/S0964-8305\(00\)00077-9](http://dx.doi.org/10.1016/S0964-8305(00)00077-9).
- Blanchette RA, Haight JE, Koestler RJ, Hatchfield PB, Arnold D. Assessment of deterioration in archaeological wood from ancient Egypt. *J Am Inst Conserv* 1994; 33:55–70. <http://dx.doi.org/10.1179/019713694806066428>.
- Blanchette RA, Held BW, Jurgens JA, McNew DL, Harrington TC, Duncan SM, et al. Wood-destroying soft rot fungi in the historic expedition huts of Antarctica. *Appl Environ Microbiol* 2004;70:1328–35. <http://dx.doi.org/10.1128/aem.70.3.1328-1335.2004>.
- Jingran G, Jian L, Jian Q, Menglin G. Degradation assessment of waterlogged wood at Haimenkou site. *Fract Struct Integr* 2014;30:495–501. <http://dx.doi.org/10.3221/JGF-ESIS.30.60>.
- Hamed SAM. *In-vitro* studies on wood degradation in soil by soft-rot fungi: *Aspergillus niger* and *Penicillium chrysogenum*. *Int Biodeter Biodegr* 2013;78:98–102. <http://dx.doi.org/10.1016/j.ibiod.2012.12.013>.
- Dutta PK, Tripathi S, Mehrotra GK, Dutta J. Perspectives for chitosan based antimicrobial films in food applications. *Food Chem* 2009;114:1173–82. <http://dx.doi.org/10.1016/j.foodchem.2008.11.047>.
- Singh T, Vesentini D, Osman A, Singh A. Mode(s) of action of chitosan: 1. The effect on fungal cell membranes. 8th Int Mycol Congr; 2006. p. 280.
- Vesentini D, Steward D, Sing A. Mode(s) of action of chitosan: 2. The effect on fungal cell wall deposition. 8th Int Mycol Congr; 2006. p. 281.
- Ravi Kumar MN. A review of chitin and chitosan applications. *React Funct Polym* 2000;46:1–27. [http://dx.doi.org/10.1016/S1381-5148\(00\)00038-9](http://dx.doi.org/10.1016/S1381-5148(00)00038-9).
- Ahonkhai EI, Arhewoh IM, Okhamafe AO. Effect of solvent type and drying method on protein retention in chitosan-alginate microcapsules. *Trop J Pharm Res* 2007;5: 583–8. <http://dx.doi.org/10.4314/tjpr.v5i2.14635>.
- Mcknight CA, Ku A, Goosen MFA, Sun D, Penney C. Synthesis of chitosan-alginate microcapsule membranes. *J Bioact Compat Polym* 1988;3:334–55. <http://dx.doi.org/10.1177/088391158800300402>.
- Guibal E. Interactions of metal ions with chitosan-based sorbents: A review. *Sep Purif Technol* 2004;38:43–74. <http://dx.doi.org/10.1016/j.seppur.2003.10.004>.
- Klug M, Sanches MNM, Laranjeira MCM, Fávère VT, Rodrigues CA. Análise das isoterms de adsorção de Cu(II), Cd(II), Ni(II) e Zn(II) pela N-(3,4-dihidroxibenil) quitosana empregando o método da regressão não linear. *Quim Nova* 1998;21: 410–3. <http://dx.doi.org/10.1590/S0100-40421998000400006>.
- Kubota N, Tatsumoto N, Sano T, Toya K. A simple preparation of half N-acetylated chitosan highly soluble in water and aqueous organic solvents. *Carbohydr Res* 2000;324:268–74. [http://dx.doi.org/10.1016/S0008-6215\(99\)00263-3](http://dx.doi.org/10.1016/S0008-6215(99)00263-3).
- Kurita K. Chitin and chitosan: Functional biopolymers from marine crustaceans. *Marine Biotechnol* 2006;8:203–26. <http://dx.doi.org/10.1007/s10126-005-0097-5>.
- Anthonsen MW, Smidsrød O. Hydrogen ion titration of chitosans with varying degrees of N-acetylation by monitoring induced $^1\text{H-NMR}$ chemical shifts. *Carbohydr Polym* 1995;26:303–5. [http://dx.doi.org/10.1016/0144-8617\(95\)00010-5](http://dx.doi.org/10.1016/0144-8617(95)00010-5).
- Rinaudo M. Chitin and chitosan: Properties and applications. *Prog Polym Sci* 2006; 31:603–32. <http://dx.doi.org/10.1016/j.progpolymsci.2006.06.001>.
- Sankararamakrishnan N, Sanghi R. Preparation and characterization of a novel xanthated chitosan. *Carbohydr Polym* 2006;66:160–7. <http://dx.doi.org/10.1016/j.carbpol.2006.02.035>.
- Yang DQ, Zhang Y, Wang X, Feng M. Fungal modifications of chitosan adhesives for manufacturing wood composites. Toronto: Fpinnovations; 2013.
- Schmidt O, Müller J, Moreth U. Potential protection effect of chitosan against wood fungi (in German). *Holz-Zentralbl* 1995;2503.
- Eikenes M, Fongen M, Roed L, Stenstrøm Y. Determination of chitosan in wood and water samples by acidic hydrolysis and liquid chromatography with online fluorescence derivatization. *Carbohydr Polym* 2005;61:29–38. <http://dx.doi.org/10.1016/j.carbpol.2005.02.006>.
- Franceschi E. X-ray diffraction in cultural heritage and archaeology studies. *OALib* 2014;1:1–10. <http://dx.doi.org/10.4236/oalib.1100437>.
- Abdel-Maksoud G, Al-Saad Z. Evaluation of cellulose acetate and chitosan used for the treatment of historical papers. *Mediterr Archaeol Archaeom* 2009;9:69–87.
- Abdel-Maksoud G. Analytical techniques used for the evaluation of a 19th century quranic manuscript conditions. *Measurement* 2011;44:1606–17. <http://dx.doi.org/10.1016/j.measurement.2011.06.017>.
- Marutoiu C, Grapini SP, Baciu A, Miclaus M, Marutoiu VC, Dreve S, et al. Scientific investigations of a 16th century stall belonging to the Evangelic Church in Bistrița, Bistrița-Năsăud county. Romania J Spectrosc 2013;2013:1–5. <http://dx.doi.org/10.1155/2013/957456>.
- Bugheanu P, Stanculescu I, Emandi I, Budrugaec P, Emandi A. The assesment of the decayed lime wood polymeric components by TG and FT-IR parameters correlation. *Int J Conserv Sci* 2010;1:211–8.
- Piccolo M, Cavallo E, Macchioni N, Pignatelli O, Pizzo B, Santoni I. Spectral characterisation of ancient wooden artefacts with the use of traditional IR techniques and ATR device: A methodological approach. *e-Preserv Sci* 2011;8:23–8.
- Gelbrich J, Mai C, Militz H. Evaluation of bacterial wood degradation by Fourier transform infrared (FTIR) measurements. *J Cult Herit* 2012;13:135–8. <http://dx.doi.org/10.1016/j.culher.2012.03.003>.
- Lo Monaco A, Marabelli M, Pelosi C, Picchio R. Colour measurements of surfaces to evaluate the restoration materials. *Proc SPIE* 2011;80840. <http://dx.doi.org/10.1117/12.889147>.
- Ozgenç O, Hiziroglu S, Yildiz UC. Weathering properties of wood species treated with different coating applications. *BioResources* 2012;7:4875–88. <http://dx.doi.org/10.15376/biores.7.4.4875-4888>.
- Benjamin CR, Raper KB, Fennell DI. The genus *Aspergillus*. *Mycologia* 1966;58:500–2. <http://dx.doi.org/10.2307/3756932>.
- Barnett H, Hunter B. Illustrated genera of imperfect fungi. 3rd ed. Minneapolis, Minnesota: Burgess publishing Co.; 1972.
- White T, Bruns T, Lee S, Taylor J. Amplification and direct sequencing of fungal ribosomal RNA genes for phylogenetics. San Diego: Academic Press; 1990.

- [34] Kimura M. A simple method for estimating evolutionary rates of base substitutions through comparative studies of nucleotide sequences. *J Mol Evol* 1980;16:111–20. <http://dx.doi.org/10.1007/BF01731581>.
- [35] Tamura K, Stecher G, Peterson D, Filipksi A, Kumar S. MEGA6: Molecular evolutionary genetics analysis version 6.0. *Mol Biol Evol* 2013;30:2725–9. <http://dx.doi.org/10.1093/molbev/mst197>.
- [36] Abdel MG. Evaluation of wax or oil/fungicide formulations for preservation of vegetable-tanned leather artifacts. *J Soc Leather Technol Chem* 2006;90:58.
- [37] Abdel-Maksoud GMM, Marcinkowska E. Evaluation of vegetable tanned-leather after artificial ageing as compared to archaeological samples. *ICOM Comm. Conserv. 12th Trienn. Meet*; 1999. p. 913.
- [38] Abdel-Maksoud G, Marcinkowska E. Changes in some properties of aged and historical parchment. *Restaurator* 2000;21:138–57. <http://dx.doi.org/10.1515/REST.2000.138>.
- [39] Billmeyer FW, Saltzman M. Principles of color technology. Wiley; 1981.
- [40] Jadoul A, Doucet J, Durand D, Pr at V. Modifications induced on stratum corneum structure after *in vitro* iontophoresis: ATR-FTIR and X-ray scattering studies. *J Control Release* 1996;42:165–73. [http://dx.doi.org/10.1016/0168-3659\(96\)01452-6](http://dx.doi.org/10.1016/0168-3659(96)01452-6).
- [41] Pouliot R, Germain L, Auger F, Tremblay N, Juhasz J. Physical characterization of the stratum corneum of an *in vitro* human skin equivalent produced by tissue engineering and its comparison with normal human skin by ATR-FTIR spectroscopy and thermal analysis (DSC). *Biochim Biophys Acta Mol Cell Biol Lipids* 1999;1439:341–52. [http://dx.doi.org/10.1016/S1388-1981\(99\)00086-4](http://dx.doi.org/10.1016/S1388-1981(99)00086-4).
- [42] Xie J, Riley C, Kumar M, Chittur K. FTIR/ATR study of protein adsorption and brushite transformation to hydroxyapatite. *Biomaterials* 2002;23:3609–16. [http://dx.doi.org/10.1016/S0142-9612\(02\)00090-X](http://dx.doi.org/10.1016/S0142-9612(02)00090-X).
- [43] Velkova V, Lafleur M. Influence of the lipid composition on the organization of skin lipid model mixtures: An infrared spectroscopy investigation. *Chem Phys Lipids* 2002;117:63–74. [http://dx.doi.org/10.1016/S0009-3084\(02\)00042-7](http://dx.doi.org/10.1016/S0009-3084(02)00042-7).
- [44] Kazarian SG, Chan KLA. Applications of ATR-FTIR spectroscopic imaging to biomedical samples. *Biochim Biophys Acta Biomembr* 1758;2006:858–67. <http://dx.doi.org/10.1016/j.bbmem.2006.02.011>.
- [45] Liao W, Wei F, Liu D, Qian MX, Yuan G, Zhao XS. FTIR-ATR detection of proteins and small molecules through DNA conjugation. *Sens Actuators B* 2006;114:445–50. <http://dx.doi.org/10.1016/j.snb.2005.06.021>.
- [46] Dias M, Naik A, Guy RH, Hadgraft J, Lane ME. *In vivo* infrared spectroscopy studies of alkanol effects on human skin. *Eur J Pharm Biopharm* 2008;69:1171–5. <http://dx.doi.org/10.1016/j.ejpb.2008.02.006>.
- [47] Rousseau W, Mitchell J, Tetteh J, Lane ME. Investigation of the permeation of model formulations and a commercial ibuprofen formulation in Carbosil® and human skin using ATR-FTIR and multivariate. *Int J Pharm* 2009;374:17–25. <http://dx.doi.org/10.1016/j.ijpharm.2009.02.018>.
- [48] Terinte N, Ibbett R, Schuster KC. Overview on native cellulose and microcrystalline cellulose I structure studied by X-ray diffraction (waxd): Comparison between measurement techniques. *Lenzinger Ber* 2011;89:118–31.
- [49] Hermans PH, Weidinger A. Quantitative investigation of the X-ray diffraction picture of some typical rayon specimens. *Text Res J* 1961;31:558–71. <http://dx.doi.org/10.1177/004051756103100607>.
- [50] Segal L, Creely JJ, Martin A, Conrad CM. An empirical method for estimating the degree of crystallinity of native cellulose using the X-ray diffractometer. *Res J* 1959;29:786–94. <http://dx.doi.org/10.1177/004051755902901003>.
- [51] Someren MK, Samson RRA, Visser J. The use of RFLP analysis in classification of the black aspergilli: Reinterpretation of the *Aspergillus niger* aggregate. *Curr Genet* 1991;19:21–6. <http://dx.doi.org/10.1007/BF00362083>.
- [52] Samson RA, Noonim P, Meijer M, Houbraken J, Frisvad JC, Varga J. Diagnostic tools to identify black aspergilli. *Stud Mycol* 2007;59:129–45. <http://dx.doi.org/10.3114/sim.2007.59.13>.
- [53] Peterson SW. Phylogenetic analysis of *Aspergillus* species using DNA sequences from four loci. *Mycologia* 2008;100:205–26. <http://dx.doi.org/10.3852/mycologia.100.2.205>.
- [54] Morrell JJ, Smith SM. Fungi colonizing redwood in cooling towers: Identities and effects on wood properties. *Wood Fiber Sci* 1988;20:243–9.
- [55] Ciolacu D, Ciolacu F, Popa V. Amorphous cellulose-structure and characterization. *Cellul Chem Technol* 2011;45:13–21.
- [56] Shang J, Yan S, Wang Q. Degradation mechanism and chemical component changes in *Betula platyphylla* wood by wood-rot fungi. *BioResources* 2013;8:6066–77. <http://dx.doi.org/10.15376/biores.8.4.6066-6077>.
- [57] Łojewska J, Miśkowiec P, Łojewski T, Proniewicz LM. Cellulose oxidative and hydrolytic degradation: In situ FTIR approach. *Polym Degrad Stab* 2005;88:512–20. <http://dx.doi.org/10.1016/j.polymdegradstab.2004.12.012>.
- [58] Poletto M, Zattera AJ, Forte MMC, Santana RMC. Thermal decomposition of wood: Influence of wood components and cellulose crystallite size. *Bioresour Technol* 2012;109:148–53. <http://dx.doi.org/10.1016/j.biortech.2011.11.122>.
- [59] Goh WN, Rosma A, Kaur B, Fazilah A, Karim AA, Bhat R. Microstructure and physical properties of microbial cellulose produced during fermentation of black tea broth (Kombucha). II. *Int Food Res J* 2012;19:153–8.
- [60] Levine AS, Fellers CR. Inhibiting effect of acetic acid upon microorganisms in the presence of sodium chloride and sucrose. *J Bacteriol* 1940;40:255–69.
- [61] Tang TKH, Schmidt O, Liese W. Environment-friendly short-term protection of bamboo against molding. *J Timber Dev Assoc India* 2009;55:8–17.
- [62] Schmidt O, Magel E, Fr uhwald A, Glukhykh L, Erdt K, Kaschurro S. Influence of sugar and starch content of palm wood on fungal development and prevention of fungal colonization by acid treatment. *Holzforschung* 2016;70:783–91. <http://dx.doi.org/10.1515/hf-2015-0181>.
- [63] Felsenstein J. Phylogenies and the comparative method. *Am Nat* 1985;125:1–15. <http://dx.doi.org/10.1086/284325>.